

Experimental evidence of dipolar interaction in bilayer nanocomposite magnets

A.J. Zambano · H. Oguchi · I. Takeuchi · J.P. Liu ·
S.E. Loffland · L.A. Bendersky · Y. Liu · Z.L. Wang

Received: 18 March 2010 / Accepted: 28 September 2010
© Springer-Verlag 2010

Abstract We use magnetic thin film hard/non-soft-magnetic trilayer systems to probe the nature of the hard–soft phase interaction and the role played by dipolar fields in one-dimensional (d) magnetic systems. We have systematically

investigated six wedge samples where the thickness of a Cu spacer layer (t_{Cu}) was gradually changed to create a varying interfacial effect on the interaction between a CoPt hard layer and a Fe soft layer. Magneto-optical Kerr effect was used to obtain the magnetization loops at 28 points on each sample, and the nucleation field (H_N) as a function of t_{Cu} was employed to characterize the layer interaction as a function of t_{Cu} . $H_N(t_{\text{Cu}})$ show a RKKY oscillatory behavior in addition to a non-negligible dipolar contribution, which had an exponential dependence. The dipolar term, which cannot be always neglected, is affected by the interface roughness and also by the CoPt crystallinity. Therefore, we cannot always consider exchange coupling to be the dominant interaction in one- d hard–soft magnetic bilayer systems, particularly, during magnetic reversal.

A.J. Zambano (✉) · H. Oguchi · I. Takeuchi
Department of Materials Science and Engineering, and Center for Superconductivity Research, University of Maryland, College Park, MD 20742, USA
e-mail: tonyza@hotmail.com
Fax: +1-301-3142029

H. Oguchi
e-mail: h.oguchi@imr.tohoku.ac.jp

I. Takeuchi
e-mail: takeuchi@umd.edu

J.P. Liu
Department of Physics, University of Texas at Arlington,
Arlington, TX 76019, USA
e-mail: pliu@uta.edu
Fax: +1-817-2723637

S.E. Loffland
Department of Physics, Rowan University, Glassboro, NJ 08028,
USA
e-mail: loffland@rowan.edu
Fax: +1-856-2564478

L.A. Bendersky
National Institute of Standards and Technology, Gaithersburg,
MD 20899, USA
e-mail: leonid.bendersky@nist.gov
Fax: +1-301-9754553

Y. Liu · Z.L. Wang
Georgia Institute of Technology, Atlanta, GA 30332-062, USA

Z.L. Wang
e-mail: zhong.wang@mse.gtech.com
Fax: +1-404-8949140

1 Introduction

Nanocomposite magnets, where a high coercive field of a hard magnet and a high magnetization of a soft magnet are combined to boost the maximum energy product ($(BH)_{\text{max}}$), represent an attractive alternative to single-phase magnets. Because of the way they are synthesized, e.g., mechanical alloying, melt spinning, etc., nanocomposite magnets typically are three-dimensional (d) structures. In constructing such systems, one important goal is to reduce the antiferromagnetic (AFM) coupling induced by the dipolar interaction between the soft and the hard phase. When the dipolar interaction is negligible, nanocomposite magnets can be considered ideal exchanged-coupled magnets, where there is only ferromagnetic (FM) interaction between the soft and hard phase [1, 2].

C. Rong et al. have used three- d micromagnetic simulations to show that the dipolar interaction can play an important role during the demagnetization process, but they also

Report Documentation Page

Form Approved
OMB No. 0704-0188

Public reporting burden for the collection of information is estimated to average 1 hour per response, including the time for reviewing instructions, searching existing data sources, gathering and maintaining the data needed, and completing and reviewing the collection of information. Send comments regarding this burden estimate or any other aspect of this collection of information, including suggestions for reducing this burden, to Washington Headquarters Services, Directorate for Information Operations and Reports, 1215 Jefferson Davis Highway, Suite 1204, Arlington VA 22202-4302. Respondents should be aware that notwithstanding any other provision of law, no person shall be subject to a penalty for failing to comply with a collection of information if it does not display a currently valid OMB control number.

1. REPORT DATE MAR 2010	2. REPORT TYPE	3. DATES COVERED 00-00-2010 to 00-00-2010	
4. TITLE AND SUBTITLE Experimental evidence of dipolar interaction in bilayer nanocomposite magnets		5a. CONTRACT NUMBER	
		5b. GRANT NUMBER	
		5c. PROGRAM ELEMENT NUMBER	
6. AUTHOR(S)		5d. PROJECT NUMBER	
		5e. TASK NUMBER	
		5f. WORK UNIT NUMBER	
7. PERFORMING ORGANIZATION NAME(S) AND ADDRESS(ES) University of Maryland, Department of Materials Science and Engineering, Center for Superconductivity Research, College Park, MD, 20742		8. PERFORMING ORGANIZATION REPORT NUMBER	
9. SPONSORING/MONITORING AGENCY NAME(S) AND ADDRESS(ES)		10. SPONSOR/MONITOR'S ACRONYM(S)	
		11. SPONSOR/MONITOR'S REPORT NUMBER(S)	
12. DISTRIBUTION/AVAILABILITY STATEMENT Approved for public release; distribution unlimited			
13. SUPPLEMENTARY NOTES			
14. ABSTRACT We use magnetic thin film hard/non/soft-magnetic trilayer systems to probe the nature of the hard?soft phase interaction and the role played by dipolar fields in onedimensional (d) magnetic systems. We have systematically investigated six wedge samples where the thickness of a Cu spacer layer (tCu) was gradually changed to create a varying interfacial effect on the interaction between a CoPt hard layer and a Fe soft layer. Magneto-optical Kerr effect was used to obtain the magnetization loops at 28 points on each sample, and the nucleation field (HN) as a function of tCu was employed to characterize the layer interaction as a function of tCu. HN(tCu) show a RKKY oscillatory behavior in addition to a non-negligible dipolar contribution, which had an exponential dependence. The dipolar term, which cannot be always neglected, is affected by the interface roughness and also by the CoPt crystallinity. Therefore, we cannot always consider exchange coupling to be the dominant interaction in one-d hard?soft magnetic bilayer systems, particularly during magnetic reversal.			
15. SUBJECT TERMS			
16. SECURITY CLASSIFICATION OF:			17. LIMITATION OF ABSTRACT
a. REPORT unclassified	b. ABSTRACT unclassified	c. THIS PAGE unclassified	Same as Report (SAR)
			18. NUMBER OF PAGES 5
			19a. NAME OF RESPONSIBLE PERSON

Table 1 CoPt/Cu(t_{Cu})/Fe(t_{Fe}). *Dep.* T is deposition temperatures, H_C is the CoPt coercivity, I is the type of interaction, D is the effective grain size of L1₀ c -axis in plane phase, H_d is the dipolar field, and

t_d is the dipolar field decay length. Uncertainties in H_d and t_d were determined by varying the fit curve in the uncertainty region of the nucleation field and t_{Cu}

Sample	CoPt Dep. T (°C)	t_{Fe} (Å)	H_C (T)	I	D (Å)	H_d (T)	t_d (Å)
1	615	30	0.13 ± 0.01	AFM	74 ± 3	0.023 ± 0.01	33 ± 15
2	615	35	0.50 ± 0.04	AFM	79 ± 10	0.058 ± 0.01	70 ± 25
3	615	15	0.70 ± 0.05	AFM	135 ± 2	0.220 ± 0.03	153 ± 100
4	620	35	0.80 ± 0.06	AFM	101 ± 2	0.105 ± 0.009	103 ± 60
5	620	40	0.95 ± 0.07	AFM	77 ± 7	0.074 ± 0.008	38 ± 20
6	615	35	1.40 ± 0.10	FM	148 ± 5		

showed that it can be adjusted by controlling the grain size of the constituent phases [3]. This consideration has been incorporated to improve experimental systems. However, reported bulk nanocomposite magnets exhibit $(BH)_{\text{max}}$ values that are far below the theoretically predicted ones. This suggests that the coupling behavior needs to be further improved. In order to achieve better results, dipolar interaction needs to be minimized or eliminated.

Traditionally, Henkel plots are used to determine the dominant type of interaction mechanism in nanocomposite magnets [3]. When a dipolar interaction is present, this method does not allow one to distinguish the main source of stray field or the exact nature of the interaction, namely soft–soft, hard–soft or hard–hard. In this work, we utilize a different approach for analyzing the dipolar interaction. We use the nucleation field (H_N) from magnetic thin film trilayer systems to probe the nature of the inter-phase interaction, the effect of non-magnetic interface impurities on soft–hard phase coupling, and the role played by the soft–hard dipolar interaction in one- d systems. We created wedge samples by inserting a non-magnetic layer with a varying thickness between soft and hard magnetic thin film layers. We use the term “sample” to denote each small region of one substrate in which the thicknesses of the non-magnetic layer is approximately constant. Simultaneous fabrication of multiple samples reduces various experimental uncertainties, such as those given by dissimilarities in growing conditions. This also makes it easier to correlate the behavior of H_N with the crystalline characteristics of the hard phase. This method provides the large amount of information necessary to delineate the subtle variation in the behavior of H_N as a function of non-magnetic layer thickness.

2 Experimental method

Six wedge samples were made on $5 \times 15 \text{ mm}^2$ MgO(110) substrates, where CoPt/Cu/Fe hard-magnetic/non-magnetic/soft-magnetic trilayers were grown by electron-beam (e-beam) evaporation [2]. The 300 Å CoPt hard magnetic layer

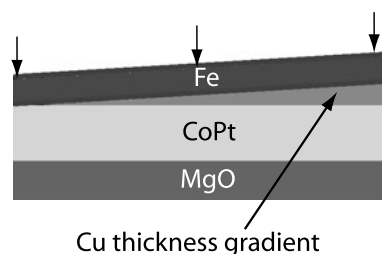


Fig. 1 Cross-sectional schematic of a wedge sample. The arrows point at three samples out of the 28 samples per wedge sample

was epitaxially grown using a 10 Å Pt buffer layer at a temperature between 615 and 620°C (Table 1). The hard layers were post-annealed at 600°C for 45 to 90 minutes typically. Then, the temperature was gradually reduced, and by 500°C the heater was turned off. We utilized the temperature gradients in the substrate holder to vary the crystallinity and the coercivity of the hard phases (Table 1). At less than 150°C, a wedged layer of Cu was deposited with thickness t_{Cu} varying between 0 and 23 Å, except for sample 1, where $0 \leq t_{\text{Cu}} \leq 49$ Å. Subsequently, the Fe soft layers were directly grown on the Cu layers with thicknesses t_{Fe} of 15, 30, or 40 Å. To prevent oxidization, the multilayers were capped by a 75 Å thick Au layer deposited at 100°C. Per wedge sample, there were 28 samples with a center-to-center separation of approximately 0.53 mm (see Fig. 1). The uncertainties in t_{Cu} were estimated as half of the difference between two consecutive samples.

We have used X-ray diffraction (XRD) to characterize the samples. With the ω -scan mode of a two-dimensional detector XRD machine, we have obtained the θ – 2θ scan by integrating over χ . XRDs were also obtained with a four-circle machine, which was also used to get the XRD patterns coming from planes that are not perpendicular to the substrate normal. The interfaces of our multilayer systems were investigated using transmission electron microscopy (TEM).

The magnetic hysteresis loop for each value of t_{Cu} was measured with a magneto-optical Kerr effect (MOKE) system. The focused spot size of the laser on samples was

less than 0.1 mm, and the rotation angle sensitivity was 5×10^{-4} degrees, which allowed us to detect small changes in magnetization as we scanned the laser spot from sample to sample on the same wedge sample. The maximal applied field was 2 T, more than sufficient to reach saturation for the hard magnetic layer.

3 Data analysis and discussion

3.1 XRD and TEM

Figure 2 shows a typical XRD pattern. The deposition of CoPt on MgO (110) by e-beam evaporation typically results in a long-range chemical ordering of the epitaxially grown $L1_0$ phase. The substrate deposition temperature determines which of the three different $L1_0$ phase orientations, one with the tetragonal c axis parallel to the substrate surface orientation ($hh0$) or two with the tetragonal c axis inclined at approximately 45° with respect to the substrate normal, orientations ($0hh$) and ($h0h$), will be predominant [4]. As expected, the analysis of the XRD data displays the presence of the (110) and (220) peaks corresponding to the $L1_0$ phase with in-plane c -axis, the (111) peak coming from a polycrystalline phase and the (202) peak corresponding to the other two epitaxial orientations. The (110) peak has a negligible contribution from the polycrystalline phase. Two extra peaks can also be observed, the Au (111) coming from the cap layer and the MgO (220) coming from the substrate [5].

The relative ratio between $L1_0$ phase orientations could not be determined because of the overlapping of the (220) and (202) peaks that could not be resolved from the 4-circle XRD data. Therefore, we characterize the CoPt hard with the effective grain size D of the $L1_0$ c -axis in-plane phase (Table 1). This is the orientation with its magnetic easy axis along the substrate plane.

D was calculated from the Sherrer's formula:

$$D = \frac{\lambda_{\alpha_1}}{W \cos \theta} \quad (1)$$

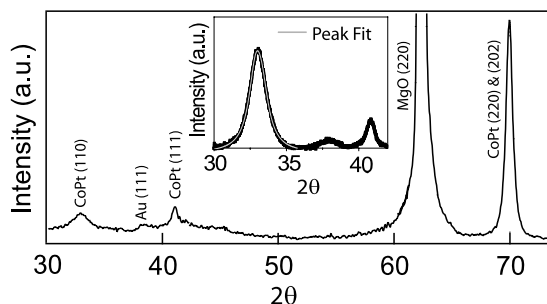


Fig. 2 Typical XRD pattern. Sample: MgO(110)/CoPt(300 Å)/Cu(t_{Cu})/Fe(30 Å)/Au(75 Å)

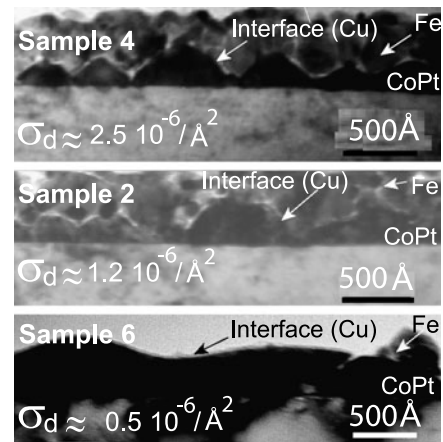


Fig. 3 TEM cross-sectional bright images. Island density $\sigma_d \approx$ (# of hills/length) [2]

where W is the full-width-at-half-maximum intensity of the (110) peak corresponding to the wavelength (λ_{α_1}) of the K_{α_1} Cu source diffractometer, and 2θ is the peak's centroid. To separate the superposition of the K_{α_1} and K_{α_2} peaks two Lorentzian functions were combined to fit the (110) peaks (inset of Fig. 2). The uncertainties in D were estimated as half of the difference between the values of D obtained with the two XRD machines.

Figure 3 displays the cross-sectional TEM images of three wedge samples. They show island-type growth of the CoPt layer. We determined the square normalized linear island-peak densities (σ_d) from the TEM images.

3.2 Hysteresis loops

An ideally coupled hard/soft magnet shows a one-phase-like magnetic hysteresis loop. On the other hand, a partially coupled magnet would exhibit a two-phase-like hysteresis loop [2]. Thus, by measuring and comparing magnetic hysteresis loops of samples of the same wedge sample, the coupling behavior can be systematically studied. From each magnetization loop, the nucleation field (H_N) was experimentally determined by the point on the curve where the drastic change in the slope takes place. This value was equated to the value of H where the tangent to the loop at the point with maximum magnetization intercepts the tangent to the loop at the point of maximum slope. In each magnetization loop, we find an upper and a lower value of H_N (inset of Fig. 4(a)). H_N was calculated by averaging their absolute values, and the uncertainty was estimated as half of their difference. H_N has the sign of the upper value.

Figure 4 displays typical examples of H_N vs. t_{Cu} data points. There is a characteristic oscillatory behavior of the CoPt and Fe layer coupling on t_{Cu} . The oscillatory behavior of H_N can be interpreted from the Ruderman–Kittel–Kasuya–Yoshida (RKKY) model [6], which explains the na-

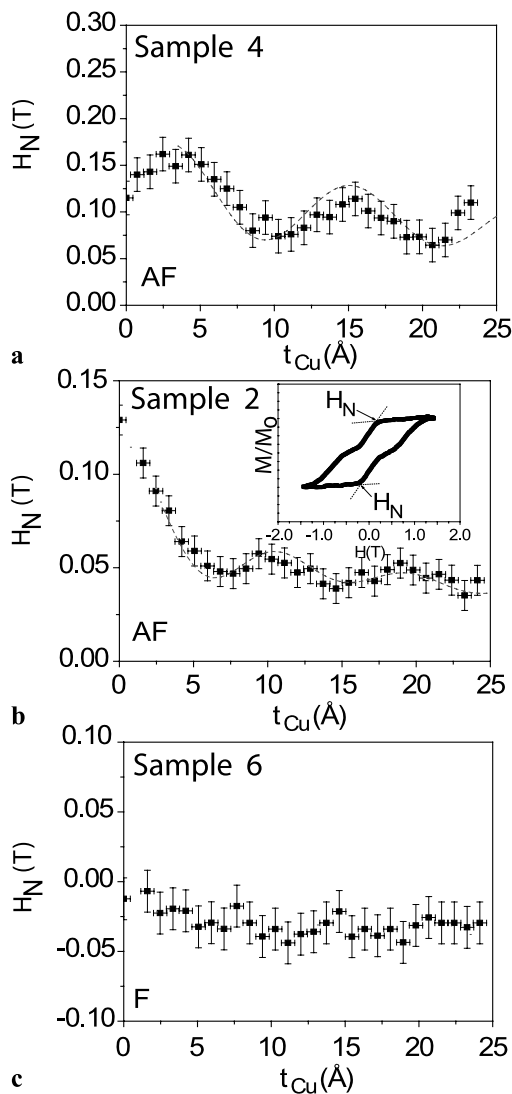


Fig. 4 Nucleation field (H_N) vs. Cu spacer thickness (t_{Cu}). Dashed gray line is the fit to (2). Inset: normalized magnetization (M/M_0) loop, graphical definition of H_N . (a) $D \approx 79$ Å, (b) $D \approx 101$ Å, and (c) $D \approx 148$ Å

ture of oscillatory exchange coupling of ferromagnet/non-magnetic spacer/ferromagnet systems with a varying non-magnetic interface spacer thickness. Figure 4(b) also shows that only 5 Å of Cu can change H_N by 60%. This indicates that a small amount of non-magnetic impurity at the interface of soft-hard magnet systems can significantly alter H_N .

The data shown in Fig. 4 are displaced along the y-axis. This cannot be directly explained by exchange coupling interaction. To understand this effect, we refer to the description given by Marguelies et al. [7]. Their interpretation is that the RKKY model can explain the oscillations, while the offset is the result of an exponential effect consequence of the presence of a large dipolar field. This field comes from a columnar granular structure with nonmagnetic grain boundaries in both layers.

Table 2 H_0 , ϕ , λ , and p are RKKY model parameters. H_0 is representative of the intensity of the exchange interaction, ϕ is related to the topology of the Fermi energy, λ is the period of the oscillations (associated to the Fermi wavelength), and p is associated with the planarity of the geometry ($p = 2$ for planar geometry) [8]. Uncertainties are not included because these parameters are presented for trend information only, and they are not crucial for the conclusion of this work

Sample	H_0 (T)	λ (Å)	ϕ	p
1	0.03	8.00	0.0	0.75
2	0.06	8.70	0.0	0.95
3	0.60	10.80	$\pi/2$	1.80
4	0.17	10.50	$\pi/2$	0.85
5	0.03	9.00	$\pi/2$	0.80

To fit the data in Fig. 4 (dashed curves), we consider that H_N consists of two terms: RKKY-like and plus an exponential decay offset term, which represents the dipolar contribution.

$$H_N(t_{Cu}) = H_0 \frac{T_e t_{Cu} / \alpha}{\sinh(T_e t_{Cu} / \alpha)} \frac{\sin(\phi + 2\pi t_{Cu} / \lambda)}{(2\pi t_{Cu} / \lambda)^p} + H_d e^{-t_{Cu} / t_d} \quad (2)$$

where $T_e = 300$ K, the constants H_0 , ϕ , p , λ , and $\alpha = 4800$ Å K characterize the RKKY-like interaction [7, 8]. H_d is the dipolar field for $t_{Cu} = 0$ and t_d is the characteristic decay length of the dipolar field. The exact functional form used for the oscillating RKKY term has little bearing on the parameters for the dipolar term, although fits are done only for $t_{Cu} > 1$ Cu monolayer, in order to avoid sensitivity to the actual form of the RKKY term. Tables 1 and 2 list the fitting parameters.

For positive values of H_N , the strong dipolar interaction favors the antiparallel alignment of the hard-soft phases (AFM coupling) (Fig. 4(a) and (b)). For negative H_N , a much weaker dipolar interaction favors the parallel alignment of the magnetic moments between the hard-soft phases (FM coupling) (Fig. 4(c)). When $H_N \leq 0$ there is a strong F interaction arising from the hard-phase pinning effect and the hard layer controls the reversal in this instance and the systems cannot be modeled by the regular RKKY theory.

3.3 Dipolar field

The combination of TEM data and the resulting fits show, as one may have expected, that H_d scales with σ_d (Fig. 5). Figure 6 suggests that there might also exist a correspondence between H_d and D . The dipolar interaction increases for increasing D up to a certain maximum and then it reduces to ≈ 0 . These experimental observations are in agreement with a simple classic electromagnetic picture, in which the dipolar field generated by an individual grain depends on

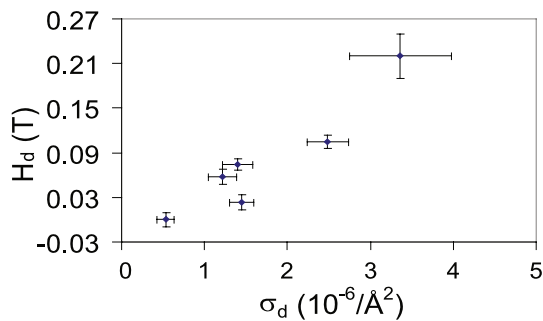


Fig. 5 Dipolar field (H_d) vs. island density (σ_d). σ_d uncertainties were calculated by propagation

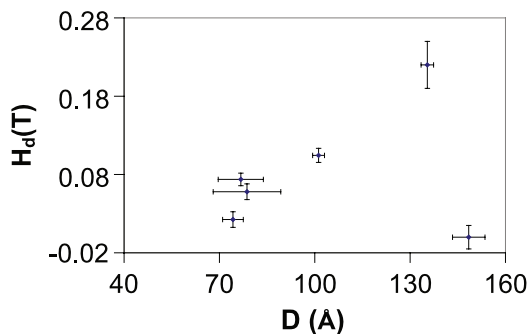


Fig. 6 Experimental data: dipolar field (H_d) vs. effective grain size of $L1_0$ phase with c -axis in plane (D)

the grain size due to the relative orientation of the magnetic poles located on the grain boundary. The fact that $D \ll$ typical island size ≈ 1000 Å (which determines σ_d) would indicate that the magnetic poles localized in the grain boundaries could also be a source of dipolar field. This grain boundary effect would add up to the σ_d effect to produce the total H_d .

High-resolution TEM images (not shown) have verified that the Fe layers were polycrystalline, suggesting that the hard phase was the main source of possible dipolar field. The polycrystalline soft phase does not contribute to the dipolar field because of its random magnetic easy-axis orientation (magnetic poles average out). On the contrary, it could contribute to separate grains as the nonmagnetic boundaries do [7].

Experimentally and theoretically, it is generally assumed that the effect of the dipolar field is negligible in one- d systems [1, 2, 9]. In addition, traditional one- d models assume that the interlayer interaction only depends on the dimensions of the soft phase. Contrary to this, the present work shows that dipolar interaction cannot only be present in one- d systems but can also strongly depend on the hard layer features.

In three- d nanocomposite magnets, especially in those systems made by compressed nanoparticles, we could expect to find polycrystalline regions or nonmagnetic grain boundaries, e.g., impurities. This would give rise to a large

dipolar field favoring the antiparallel alignment of the hard-soft phases. Independently of the hard-phase material, the way to reduce this effect is by increasing the hard-phase effective grain size and reducing the non-magnetic grain boundary and non-magnetic regions between hard and soft phases.

4 Conclusion

In summary, we have systematically investigated thickness gradient effects of a Cu interface layer on the interaction between a CoPt hard magnetic, grown at 615 and 620°C, and a Fe soft layer. We have observed a RKKY-oscillatory behavior of H_N vs. t_{Cu} with decreasing amplitude in addition to an exponential decay. The latter is a consequence of the presence of the dipolar interaction in nanocomposite magnets. We also found that a small amount of non-magnetic impurity (~ 5 Å in thickness), at the interface of soft-hard magnet systems, can significantly alter H_N (by as much as 60%). A correlation between the effective grain size of the CoPt $L1_0$ phase with the tetragonal c -axis in plane and the dipolar interaction was observed. This suggests that besides the interface roughness, another factor that might determine the dipolar interaction is the effective grain size and non-magnetic or polycrystalline grain boundary of the hard phase. (Only for hard phases with large or very small grain sizes, dipolar interaction is negligible.) Therefore, to reduce dipolar effects in nanocomposite magnets, the hard-phase effective grain size must be increased, and the roughness as well as the volume of the non-magnetic regions between hard and soft phases must be minimized.

Acknowledgements This work was supported by ONR/MURI under Grant No. N00014-05-1-0497 and NSF DMR 0231291.

References

1. H. Zeng, J. Li, J.P. Liu, Z.L. Wang, S. Sun, *Nature* **420**, 395–398 (2002)
2. A.J. Zambano, H. Oguchi, I. Takeuchi, Y. Choi, J.S. Jiang, J.P. Liu, S.E. Lofland, D. Josell, L.A. Bendersky, *Phys. Rev. B* **75**(14), 144429 (2007) and references therein
3. C. Rong, H. Zhang, R. Chen, S. He, B. Shen, *J. Magn. Magn. Mater.* **302**, 126–136 (2006) and references therein
4. M. Yu, H. Oguchi, I. Takeuchi, J.P. Liu, D. Josell, L.A. Bendersky, A.J. Zambano, *Mater. Sci. Eng. B* **142**, 139 (2007)
5. P. Bruno, C. Chappert, *Phys. Rev. Lett.* **67**, 1602 (1991)
6. H. Oguchi, A. Zambano, M. Yu, J. Hattrick-Simpers, D. Banerjee, Y. Liu, Z.L. Wang, J.P. Liu, S.E. Lofland, D. Josell, I. Takeuchi, *J. Appl. Phys.* **105**, 023912 (2009)
7. D.T. Margulies, M.E. Schabes, W.Mc. Chesney, E.E. Fullerton, *Appl. Phys. Lett.* **80**, 91 (2002)
8. S.S.P. Parkin, D. Mauri, *Phys. Rev. B* **44**, 7131 (1991)
9. S.T. Chui, *J. Appl. Phys.* **85**, 4397 (1999)